Sciencexpress Research Article

Kepler-9: A System of Multiple Planets Transiting a Sun-Like Star, Confirmed by Timing Variations

Matthew J. Holman,[1]* Daniel C. Fabrycky,[1] Darin Ragozzine,[1] Eric B. Ford,[2] Jason H. Steffen,[3] William F. Welsh,[4] Jack J. Lissauer,[5,6] David W. Latham,[1] Geoffrey W. Marcy,[7] Lucianne M. Walkowicz,[7] Natalie M. Batalha,[8] Jon M. Jenkins,[9] Jason F. Rowe,[5,20] William D. Cochran,[10] Francois Fressin,[1] Guillermo Torres,[1] Lars A. Buchhave,[1,11] Dimitar D. Sasselov,[1] William J. Borucki,[5] David G. Koch,[5] Gibor Basri,[7] Timothy M. Brown,[13,21] Douglas A. Caldwell,[5,9] David Charbonneau,[1] Edward W. Dunham,[14] Thomas N. Gautier III,[15] John C. Geary,[1] Ronald L. Gilliland,[16] Michael R. Haas,[5] Steve B. Howell,[17] David R. Ciardi,[11] Michael Endl,[10] Debra Fischer,[18] Gábor Fürész,[1] Joel D. Hartman,[1] Howard Isaacson,[7] John A. Johnson,[19] Phillip J. MacQueen,[10] Althea V. Moorhead,[2] Robert C. Morehead,[2] Jerome A. Orosz[4]

[1]Harvard-Smithsonian Center for Astrophysics, 60 Garden Street, Cambridge, MA 02138, USA. [2]University of Florida, Gainesville, FL 32611, USA. [3]Fermilab Center for Particle Astrophysics, Batavia, IL 60510, USA. [4]San Diego State University, San Diego, CA 92182, USA. [5]NASA Ames Research Center, Moffett Field, CA 94035, USA. [6]Stanford University, Stanford, CA 94305, USA. [7]University of California, Berkeley, CA 94720, USA. [8]San Jose State University, San Jose, CA 95192, USA. [9]SETI Institute, Mountain View, CA 94043, USA. [10]University of Texas, Austin, TX 78712, USA. [11]Niels Bohr Institute, Copenhagen University, DK-2100 Copenhagen, Denmark. [12]NASA Exoplanet Science Institute/California Institute of Technology, Pasadena, CA 91125, USA. [13]Las Cumbres Observatory Global Telescope, Goleta, CA 93117, USA. [14]Lowell Observatory, Flagstaff, AZ 86001, USA. [15]Jet Propulsion Laboratory/California Institute of Technology, Pasadena, CA 91109, USA. [16]Space Telescope Science Institute, Baltimore, MD 21218, USA. [17]National Optical Astronomy Observatory, Tucson, AZ 85719, USA. [18]Yale University, New Haven, CT 06510, USA. [19]California Institute of Technology, Pasadena, CA 91125, USA. [20]NASA Postdoctoral Program Fellow. [21]University of California, Santa Barbara, CA 93106, USA.

*To whom correspondence should be addressed. E-mail: mholman@cfa.harvard.edu

The Kepler spacecraft is monitoring over 150,000 stars for evidence of planets transiting those stars. We report the detection, based on seven months of Kepler observations, of two Saturn-size planets that transit the same Sun-like star. Their 19.2- and 38.9-day periods are presently increasing and decreasing at respective average rates of 4 and 39 minutes per orbit, and in addition the transit times of the inner body display an alternating variation of smaller amplitude. These signatures are characteristic of gravitational interaction of two planets near a 2:1 orbital resonance. Six radial velocity observations show that these two planets are the most massive objects orbiting close to the star and substantially improve the estimates of their masses. After removing the signal of the two confirmed giant planets, we identify an additional transiting super-Earth-size planet candidate with a period of 1.6 days.

Introduction. The Kepler mission was designed to measure the frequency of Earth-size planets in the habitable zones of Sun-like stars, by observing the dimming of star light when a planet passes in front of (i.e., transits) its parent star (*1*). Transiting planets are particularly valuable, because their photometry, in conjunction with radial velocity observations, yields the planets' physical properties (e.g., radius, mass, and density) (*2*, *3*). Kepler has identified over 700 transiting planet candidates (*4*), including some systems with multiple transiting exoplanet candidates (*5*). Confirming that each of these candidates is actually a planet (as opposed to various astrophysical false positives, e.g. diluted eclipsing binaries) requires extensive follow-up observations. We report the detection of a system of two transiting planets (Kepler-9 b and c) showing transit timing variations (TTVs) (*6*, *7*).

Kepler photometry. The Kepler data pipeline identified two transiting planet candidates orbiting a star now designated Kepler-9 (KIC 3323887, 2MASS 19021775+3824032, KOI-377) and performed a series of checks to exclude common false positives (*8*–*10*). The Kepler photometric observations of Kepler-9 reported here span 13 May 2009 to 16 December 2009 UT and consist of a nearly continuous series of 29.426 min exposures through a broad optical bandpass (*1*). Because preliminary estimates of the transit times suggested that the transit times were not strictly periodic, this system was selected for intensive study.

The Kepler light curves (Figs. 1 and 2) show that Kepler-9 is a mildly active star, with photometric variations somewhat larger than those exhibited by the active Sun. The light curves show the effects of stellar spots (radius ~0.1 R_*, where R_* is

the stellar radius) and a stellar rotation period of ~16.7 d. Ground-based telescopic observations established that the properties of the host star are quite similar to those of the Sun (see Supporting Online Material, hereafter SOM).

Transit timing variations. The orbital periods of the two planet candidates are approximately 19.24 (Kepler-9b) and 38.91 (Kepler-9c) days. We modeled each transit separately, allowing for variations in the transit time, duration, depth, and shape. Because there are substantial variations in the transit times, but not in any of the other parameters, we determined the final transit times by fitting a detailed transit model, requiring a common transit duration, depth, and shape for each planet candidate, but fitting for the mid-time of each transit (Fig. 3 and tables S4 and S5). The observed changes are much larger than the ~80-s uncertainty with which we measured the times of transit, as well as the expected variations due to a planet transiting stellar spots (SOM).

At BJD 2455088.212 (the weighted average of the transit times), the ratio of the best-fit orbital periods is Pc/Pb = 2.023, indicating the system is likely affected by a 2:1 mean motion resonance (MMR). Resonance libration can cause the instantaneous period ratio to differ by a few percent from the long-term average ratio, even if the planets are well within the resonance. For planets in a 2:1 MMR, conservation of energy, assuming no strong scattering and slow variation of the orbital elements, implies that the period derivatives have opposite sign with a ratio dependent on the planet-planet mass ratio. We measure $-[(\Delta P_b/P_b)/(\Delta P_c/P_c)] = 0.375$, suggesting a mass ratio of $M_c/M_b \approx 0.6$ (see SOM). In addition to the slow change in orbital period, the times between successive pairs of transits of Kepler-9b also show an alternating pattern with an amplitude of 2 to 4 minutes (Fig. 3). This "chopping" signal is due to the alternating position of the outer planet at the time of transit of the inner planet, and it scales with the mass of the outer body. These interdependent timing variations indicate that the two bodies are gravitationally interacting and thus must be orbiting the same star.

Dynamical model. The observed transit timing variations are the natural consequences of a system of two planets orbiting near the 2:1 MMR. We verified this by numerically simulating a fully interacting 3-body system composed of a star of mass 1.0 $M_\odot$ and two planets. We fit the planet masses and orbits by comparing the transit times and durations predicted by the numerical model with those observed (Fig. 4).

Based on the photometry alone, we exclude masses for Kepler-9b less than 0.02 M_{Jup} and greater than 4 M_{Jup}, and for Kepler-9c less than 0.03 M_{Jup} and greater than 2 M_{Jup}, at the 3-σ level (Fig. 4). This confirms that these are two planet-mass objects orbiting a Sun-like star and that their eccentricities are small ($\lesssim 0.2$). We verified that for masses for Kepler-9b and 9c that correspond to brown dwarfs or stars, the fits to the transit times and durations are very poor, and the systems are dynamically unstable on time scales of tens of years.

Using the times and durations of transits observed over the lifetime of the Kepler mission, we expect that the TTVs alone will constrain the masses, eccentricities, and mutual inclination of the two established planets with substantially reduced uncertainties (SOM). Nevertheless, we obtained a few strategically timed high-precision radial velocity (RV) measurements with the HIRES (*13*) instrument on the 10m Keck 1 telescope (SOM). Assuming that the RVs are dominated by Kepler-9b and Kepler-9c, we infer masses of 0.252 ± 0.013 M_{Jup} and 0.172 ± 0.013 M_{Jup} for Kepler-9b and Kepler-9c (Table 1), based on the combination of RVs, transit times, and durations (Fig. 4, dashed line). Figure 3 shows the RVs predicted by the model and those observed (these were included in the fit).

The measured ratio of transit durations is consistent with both planets transiting the same star with low-eccentricity orbits and similar impact parameters. While the inclination of each planet's orbit relative to the plane of the sky ($i_{b,sky}$, $i_{c,sky}$) is measured from the transit duration and shape, the relative inclination between the orbits depends on the difference in the longitudes of ascending node ($\Delta\Omega_{sky}$). In general, dynamical interactions induce nodal precession that in turn causes a drift in the impact parameter and the duration of the transits (*14*, *15*). The lack of transit duration variations provides a constraint on the mutual inclinations and the presence of moons (*14*). Multiple transiting planets are most likely to be seen in systems with small relative orbital inclinations. For the orbital periods of Kepler-9 b and c, the probability of both planets transiting decreases rapidly as the relative inclination increases beyond 2º (*16*). The current observations favor a small relative inclination ($\lesssim 10^\circ$).

Follow-up observations. We performed a series of tests to exclude a variety of astrophysical configurations that could mimic the transits seen in the Kepler photometry. High-resolution imaging revealed that Kepler-9 has three neighboring stars located within 8 arcsec of it, implying minor contamination ($\lesssim 1$ %) of the transit depth (*12*). Because all identified neighbors are ≥3.7 magnitudes fainter, none could mimic the Kepler-9b or Kepler-9c transits, even if it were an eclipsing binary that dimmed by 50%. Moreover, the likelihood is negligible that the two transit signatures having a period ratio of 2:1 could be caused by stellar-mass companions, as this configuration would not be stable (*11*). Modeling of an exhaustive variety of stellar blend scenarios (*12*), assuming the photometry of each planet candidate is the result of the brightness variations of an eclipsing binary being diluted by the brighter candidate star, has shown that, in the case of Kepler-9b and Kepler-9c, the only blends that could

reproduce the Kepler light curve would be within 2 magnitudes of the target brightness. A combination of high-resolution imaging and spectroscopic constraints rules out these scenarios and provides an independent confirmation of the planetary status of the two planets.

Super-Earth-size candidate. After filtering out the transits of Kepler-9b and Kepler-9c, there is evidence for a third, smaller planet candidate with a period of 1.5925 days and transit depth of ~200 ppm (Fig. 6). Until it is confirmed as a planet (as opposed to a background eclipsing binary), we refer to this body as KOI-377.03, following the internal enumeration of Kepler Objects of Interest (KOI). Because the transit depth of KOI-377.03 is similar to the scatter in each 30-minute observation, individual events are difficult to distinguish, but the transit light curve is very significant in binned photometry (Fig. 5). The transit duration (~2.8 hours) is consistent with a central transit of the same star orbited by Kepler-9b and Kepler-9c (which transit with a larger impact parameter). If this is a planet orbiting the same star, it would have a radius of ~1.5$R_{\oplus}$, making KOI-377.03 one of the smallest planets detected to date. We verified with *n*-body integrations that a system composed of Kepler-9, Kepler-9b, Kepler-9c, and KOI-377.03 (assuming an Earth-like density for the KOI-377.03) is dynamically stable for at least the time scale of the numerical integrations (SOM).

If KOI-377.03 is a planet in the same system, its expected TTV amplitude is only tens of seconds (*7*), which is not surprising given the large period ratio (12.1) between KOI-377.03 and Kepler-9b. Neither this signal, nor the TTVs induced on Kepler-9b or Kepler-9c from KOI-377.03, are likely to be measured by Kepler. However, the expected radial velocity signature from such a planet would be ~1.5 m/s semi-amplitude (using an Earth-like density) and may be contributing to the observed RV scatter.

Discussion. The detailed dynamics of a resonant system probes the system's formation. Resonant systems of giant planets inside the snow line most likely formed outside of resonance and at larger distances. Slow, smooth differential migration through the system's natal disk naturally leads to planets becoming trapped in the 2:1 MMR with small amplitude libration of resonant angles, as is the case for the GJ876 system (*17*, *18*). Although several other planetary systems are near the 2:1 MMR (*19–23*), or show more complicated resonance structure (*24*), measuring the libration amplitude of resonant angles from radial velocity observations is challenging even for the most favorable system (*24*, *25*). For multi-transiting systems on the other hand, resonant angles can be accurately measured via TTVs (*26*). For the Kepler-9 system, the expected libration period, based on numerical simulations, is ~4 years.

The best-fit Kepler-9 b and c model is dynamically stable for over 2.7 billion years, but only one of the resonant angles librates. For nearby, stable solutions each of the resonant angles circulate. Large libration amplitude (Fig. 4, bottom panel) could be due to a more rapid migration (*27*) or excitation after resonant capture. For example, continued migration following resonant capture can lead to eccentricity excitation and eventually planet-planet scattering (*28–31*). Other mechanisms such as turbulence in the protoplanetary disk (*32*), scattering of planetesimals (*33*, *34*), and perturbations by other planets (*35*) could also be responsible for a large libration amplitude. In principle, each of these mechanisms could perturb a resonant system so as to increase the libration amplitude. For Kepler-9 b and c tidal dissipation is expected to be too slow to have broken the MMR (*36*).

Our models currently indicate a solar-mass star with a radius of ~1.1 $R_{\odot}$, based on the observed durations and impact parameters (SOM). Combining this with the well-measured radius ratio, the two planets Kepler-9 b and c have nearly identical radii of ~0.8 R_{Jup}. The best-fit planet masses and radii are slightly smaller than those of Saturn. Theoretical models indicate that such planets are composed primarily of H and He (*37–39*).

The equilibrium temperatures for Kepler-9 b and c are ~740 K and ~540 K, respectively (assuming Bond albedos of 0.2). The mass-radius relation is insensitive to the equilibrium temperatures, but these could be affected by a young age (*38*). The heavy element fractions of Kepler-9 b and c are indeterminate (~ 0.1 to 0.8), but core-less (metal-free) models seem excluded.

KOI-377.03 might correspond to a super-Earth-size planet of radius ~1.5$R_{\oplus}$. With no additional information available for this planet, the upper mass limit of 7$M_{\oplus}$ corresponds to the maximum mantle stripping limit for a maximally iron-rich super-Earth (*40*). The lower mass limit is less clear—it could be as small as 1$M_{\oplus}$ for a volatile-rich planet with a hot extended atmosphere, e.g., water steam (*41*, *42*). The planet candidate is so close to its host star, comparable to CoRoT-7b, that its ~2200 K estimated surface temperature is very high, and volatile-rich solutions are less likely if the Kepler-9 planetary system is old and evaporation has been significant. A volatile-poor rocky KOI 377.03 super-Earth with Ganymede-like Fe/Si ratio, would correspond to a planet mass of ~3.5 $M_{\oplus}$ (*43*). Such a planet would have formed volatile-rich, only to lose all its water due to evaporation.

References and Notes

1. D. G. Koch *et al*., *Astrophys. J.* **713**, L79 (2010).
2. D. Charbonneau, T. M. Brown, A. Burrows, G. Laughlin, *Protostars and Planets V*, pp. 701–716 (2007).
3. J. N. Winn, *IAU Symposium* (2009), vol. 253 of *IAU Symposium*, pp. 99–109.
4. W. J. Borucki *et al*., *Astrophys. J.*, preprint available at http://arxiv.org/abs/1006.2799.

5. J. H. Steffen *et al*., *Astrophys. J.*, preprint available at http://arxiv.org/abs/1006.2763.
6. E. Agol, J. Steffen, R. Sari, W. Clarkson, *Mon. Not. R. Astron. Soc.* **359**, 567 (2005).
7. M. J. Holman, N. W. Murray, *Science* **307**, 1288 (2005).
8. J. M. Jenkins *et al*., *Astrophys. J.* **713**, L87 (2010).
9. D. A. Caldwell *et al*., *Astrophys. J.* **713**, L92 (2010).
10. N. M. Batalha *et al*., *Astrophys. J.* **713**, L103 (2010).
11. L. G. Kiseleva, P. P. Eggleton, V. V. Orlov, *Mon. Not. R. Astron. Soc.* **270**, 936 (1994).
12. G. Torres *et al*., ArXiv e-prints (2010).
13. S. S. Vogt *et al*., *Society of Photo-Optical Instrumentation Engineers (SPIE) Conference Series*, D. L. Crawford, E. R. Craine, Eds. (1994), vol. 2198 of *Society of Photo-Optical Instrumentation Engineers (SPIE) Conference Series*, pp. 362.
14. J. Miralda-Escudé, *Astrophys. J.* **564**, 1019 (2002).
15. S. Ballard *et al*., *Astrophys. J.* **716**, 1047 (2010).
16. D. Ragozzine, M. J. Holman, *Astrophys. J.*, preprint available at http://arxiv.org/abs/1006.3727.
17. J. J. Lissauer, *Nature* **409**, 23 (2001).
18. M. H. Lee, S. J. Peale, *Astrophys. J.* **567**, 596 (2002).
19. G. W. Marcy *et al*., *Astrophys. J.* **581**, 1375 (2002).
20. M. Mayor *et al*., *Astron. Astrophys.* **415**, 391 (2004).
21. S. S. Vogt *et al*., *Astrophys. J.* **632**, 638 (2005).
22. C. G. Tinney *et al*., *Astrophys. J.* **647**, 594 (2006).
23. F. Pepe *et al*., *Astron. Astrophys.* **462**, 769 (2007).
24. E. J. Rivera *et al*., *Astrophys. J.*, preprint available at http://arxiv.org/abs/1006.4244.
25. A. C. M. Correia *et al*., *Astron. Astrophys.* **511**, A21 (2010).
26. S. Meschiari *et al*., *Pub. Astron. Soc. Pac.* **121**, 1016 (2009).
27. M. H. Lee, *Astrophys. J.* **611**, 517 (2004).
28. Z. Sándor, W. Kley, *Astron. Astrophys.* **451**, L31 (2006).
29. Z. Sándor, W. Kley, P. Klagyivik, *Astron. Astrophys.* **472**, 981 (2007).
30. A. T. Lee, E. W. Thommes, F. A. Rasio, *Astrophys. J.* **691**, 1684 (2009).
31. F. Marzari, C. Baruteau, H. Scholl, *Astron. Astrophys.* **514**, L4 (2010).
32. F. C. Adams, G. Laughlin, A. M. Bloch, *Astrophys. J.* **683**, 1117 (2008).
33. R. A. Murray-Clay, E. I. Chiang, *Astrophys. J.* **651**, 1194 (2006).
34. A. Morbidelli, K. Tsiganis, A. Crida, H. F. Levison, R. Gomes, *Astron. J.* **134**, 1790 (2007).
35. D. C. Fabrycky, R. A. Murray-Clay, *Astrophys. J.* **710**, 1408 (2010).
36. C. Terquem, J. C. B. Papaloizou, *Astrophys. J.* **654**, 1110 (2007).
37. I. Baraffe, Y. Alibert, G. Chabrier, W. Benz, *Astron. Astrophys.* **450**, 1221 (2006).
38. J. J. Fortney, M. S. Marley, J. W. Barnes, *Astrophys. J.* **659**, 1661 (2007).
39. S. Seager, M. Kuchner, C. A. Hier-Majumder, B. Militzer, *Astrophys. J.* **669**, 1279 (2007).
40. R. A. Marcus, D. Sasselov, L. Hernquist, S. T. Stewart, *Astrophys. J.* **712**, L73 (2010).
41. D. Valencia, D. D. Sasselov, R. J. O'Connell, *Astrophys. J.* **665**, 1413 (2007).
42. L. A. Rogers, S. Seager, *Astrophys. J.* **712**, 974 (2010).
43. L. Zeng, S. Seager, *Pub. Astron. Soc. Pac.* **120**, 983 (2008).
44. Funding for this Discovery mission is provided by NASA's Science Mission Directorate. We acknowledge NASA Cooperative Agreement NCC2-1390. D.C.F. acknowledges support from the Michelson Fellowship, supported by the National Aeronautics and Space Administration and administered by the NASA Exoplanet Science Institute. This work is based in part on observations obtained at the W. M. Keck Observatory, which is operated by the University of California and the California Institute of Technology. Some of the observations used in this paper were obtained at Kitt Peak National Observatory, National Optical Astronomy Observatory, which is operated by the Association of Universities for Research in Astronomy (AURA) under cooperative agreement with the National Science Foundation.

Supporting Online Material

www.sciencemag.org/cgi/content/full/science.1195778/DC1
SOM Text
Figs. S1 to S4
Tables S1 to S6
References

28 July 2010; accepted 19 August 2010
Published online 26 August 2010; 10.1126/science.1195778
Include this information when citing this paper.

Fig. 1. The raw photometry of Kepler-9 (KOI-377, KIC 3323887) showing data from Quarters 1-3. The jumps in flux correspond to the breaks between quarters, when Kepler-9 moves to a different detector after the rotation of the spacecraft.

Fig. 2. The detrended light curve of Kepler-9 (KOI-377, KIC 3323887), clearly showing two periodic transit signals well above the typical scatter of ~210 ppm. This was the light curve used to derive the results described in this paper. Kepler-9b, with period near 19.2 days, is the slightly deeper transit, with the third and seventh transits missing (due to

incomplete duty cycle). Kepler-9c, with a period near 39 days, is a little shallower, and all transits are observed. At this scale, the light curve of the third candidate, KOI-377.03, is not apparent.

Fig. 3. (Top) Offset of the observed transit times for planets "b" (blue x symbols) and "c" (red dot symbols) compared to those calculated with linear ephemerides, quadratic ephemerides, and a dynamical model (diamonds) in which the planets fully interact. These calculations display the best-fit model (SOM table S1). Only the diamond symbols are shown for events for which Kepler data were not available. (Bottom) A comparison of the observed radial velocity (dots) with that predicted by the dynamical model (solid line and diamonds).

Fig. 4. Fits to the transit timing observations as a function of assumed Mc. (Top) The χ^2 statistic, where the transit mid-times and durations are fit (solid) and where the transit mid-times, transit durations, and the radial velocities are also fit (dashed). (Middle) The ratio of planetary masses, showing that for small masses, the mass ratio can be predicted from the ratio of the quadratic terms in the transit time ephemerides. (Bottom) The full amplitude of the 2:1 resonance angle $\theta_1 = 2\lambda_c - \lambda_b - \varpi_b$ in a 10^3 year integrations. Upward-pointing triangles indicate circulation of the resonance angle.

Fig. 5. Light curves for Kepler-9b (top panel) and Kepler-9c (bottom panel). In each panel, the top curve shows the detrended Kepler photometry (points, colored by transit epoch) folded with the best-fit period. Significant displacements are due to the large transit timing variations caused by gravitational interactions between the planets, as described in the text. The bottom curve in each panel (displaced downward for clarity) shows the transits shifted to a common center using the measured transit times (SOM), giving depths of ~7 millimagnitudes and durations of ~4.5 hours. Also shown are solid lines (also colored by transit epoch) from the full numerical-photometric model, folded or shifted in the same way as the data.

Fig. 6. The detrended relative photometry of Kepler-9, folded on its orbital period, showing the full phase curve and the signal due to candidate KOI-377.03. For this we adopt an ephemeris for KOI-377.03 of BJD 2454965.74 + E×1.5925. This light curve could be due to an astrophysical false positive, although the transit parameters and other considerations are consistent with this candidate being a co-planar third planet in the Kepler-9 system. Vertical lines show phased photometry binned every ~15 minutes with error bars taken from the scatter of the data in each bin. Also shown is a model for the central transit of a planet with radius ~1.5$R_\oplus$.

Table 1. Parameters for Kepler-9, Kepler-9b, and Kepler-9c based on the combined fit to the observed transit times, transit durations, and radial velocities. The quadratic ephemerides for both planets are approximations to the actual transit times and are not meant to be extrapolated beyond the observations presented in this paper. The quoted uncertainties in the planetary masses, radii, densities, and semimajor axes do not incorporate the uncertainty in the stellar mass.

Stellar parameters	**Value**
Mass M_* ($M_\odot$)	1.0 ± 0.1
Radius R_* ($R_\odot$)	1.10 ± 0.09
Planet "b" parameters	**Value**
Ephemeris (BJD)	$(2455073.43381 \pm 0.00052)$ $+(19.243159 \pm 0.000098)N$ $+(0.001274 \pm 0.000036)N^2$
Transit duration (days)	0.15927 ± 0.00044
Scaled planet radius Rp/R_*	0.07885 ± 0.00081
Scaled impact parameter b/R_*	0.654 ± 0.033
Mass Mp ($MJup$)	0.252 ± 0.013
Radius Rp($RJup$)	0.842 ± 0.069
Density ρp (g/cc)	0.524 ± 0.132
Orbital semimajor axis a (AU)	0.140 ± 0.001
Planet "c" parameters	**Value**
Ephemeris (BJD)	$(2455164.18301 \pm 0.00074)$ $+(38.908610 \pm 0.000738)N$ $-(0.013452 \pm 0.000147)N^2$
Transit duration (days)	0.17121 ± 0.00057
Scaled planet radius Rp/R_*	0.07708 ± 0.00080
Scale impact parameter b/R_*	0.716 ± 0.026
Mass Mp ($MJup$)	0.171 ± 0.013
Radius Rp($RJup$)	0.823 ± 0.067
Density ρp (g/cc)	0.383 ± 0.098
Orbital semimajor axis a (AU)	0.225 ± 0.001

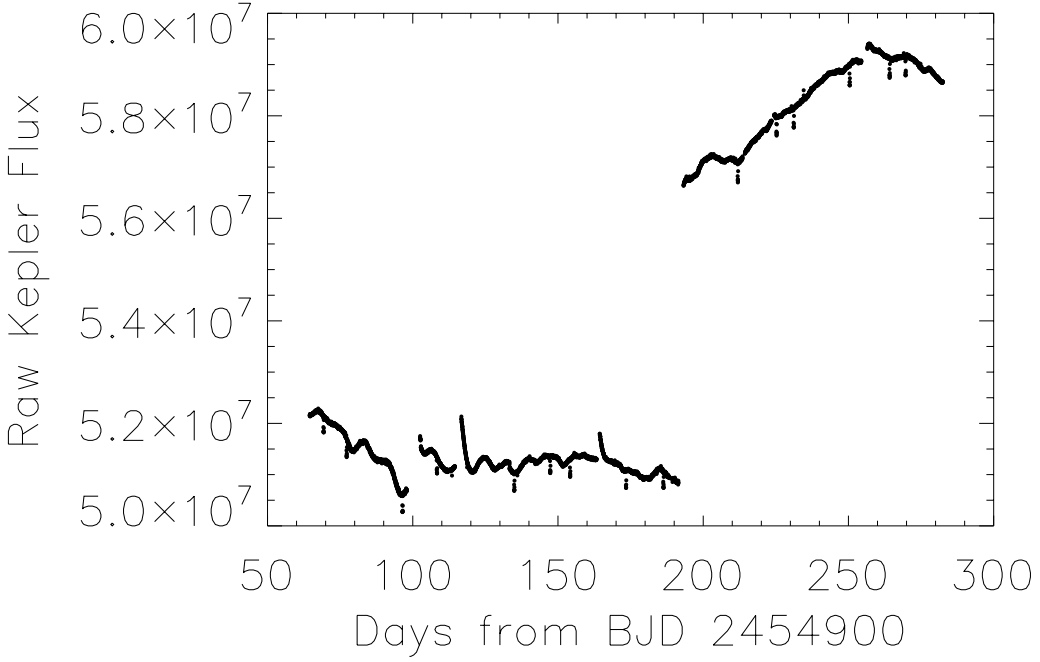
6.0×10^7
5.8×10^7
5.6×10^7
5.4×10^7
5.2×10^7
5.0×10^7
Raw Kepler Flux
50
100
150
200
250
300
Days from BJD 2454900

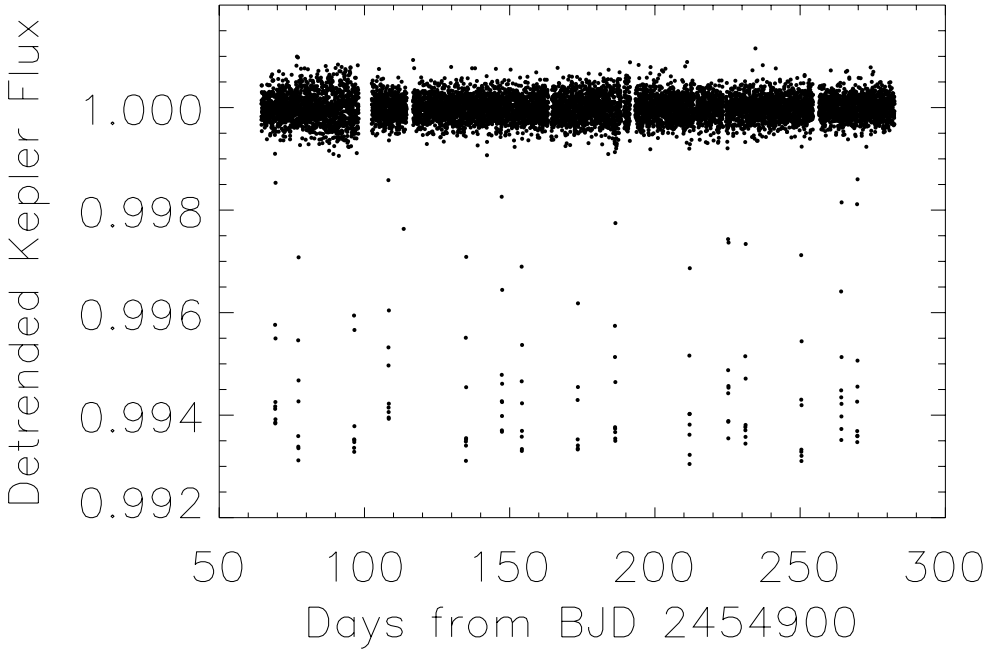
Detrended Kepler Flux
1.000
0.998
0.996
0.994
0.992
50
100
150
200
250
300
Days from BJD 2454900

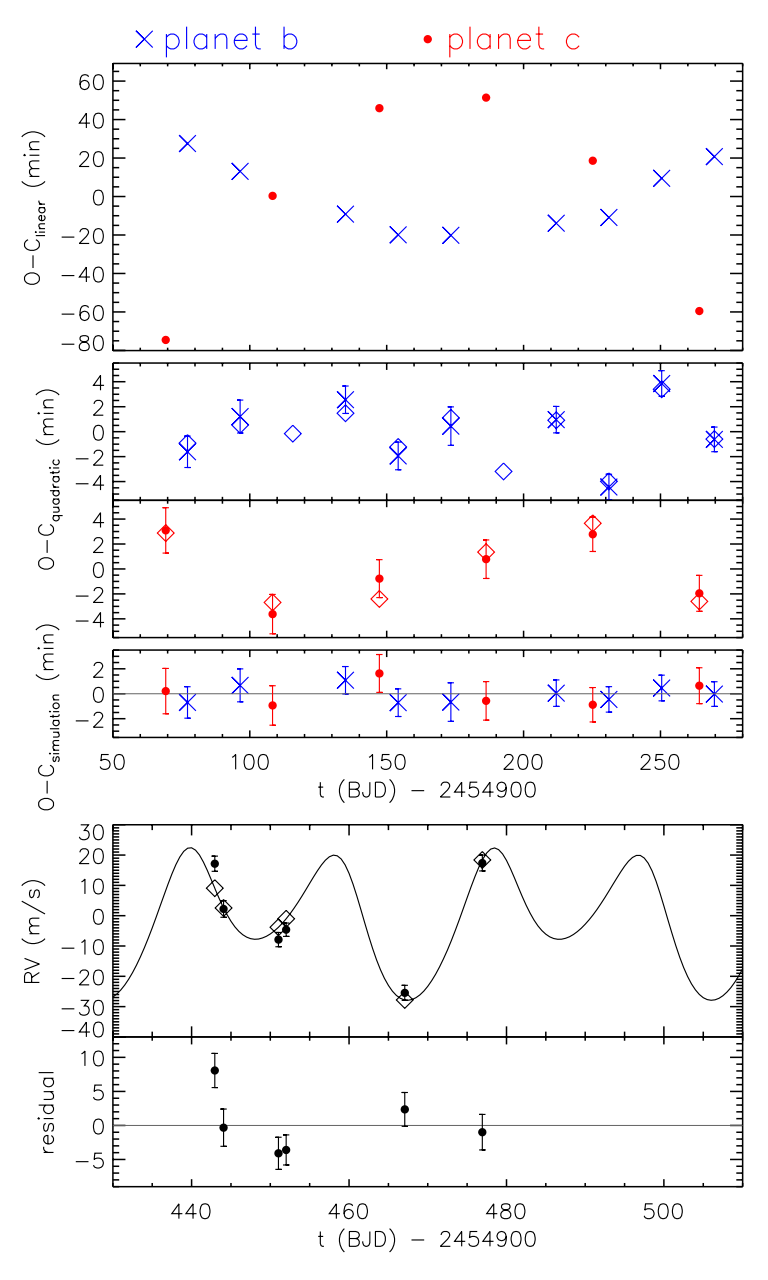
planet b
planet c
O−C_linear (min)
O−C_quadratic (min)
O−C_simulation (min)
t (BJD) − 2454900
RV (m/s)
residual
t (BJD) − 2454900

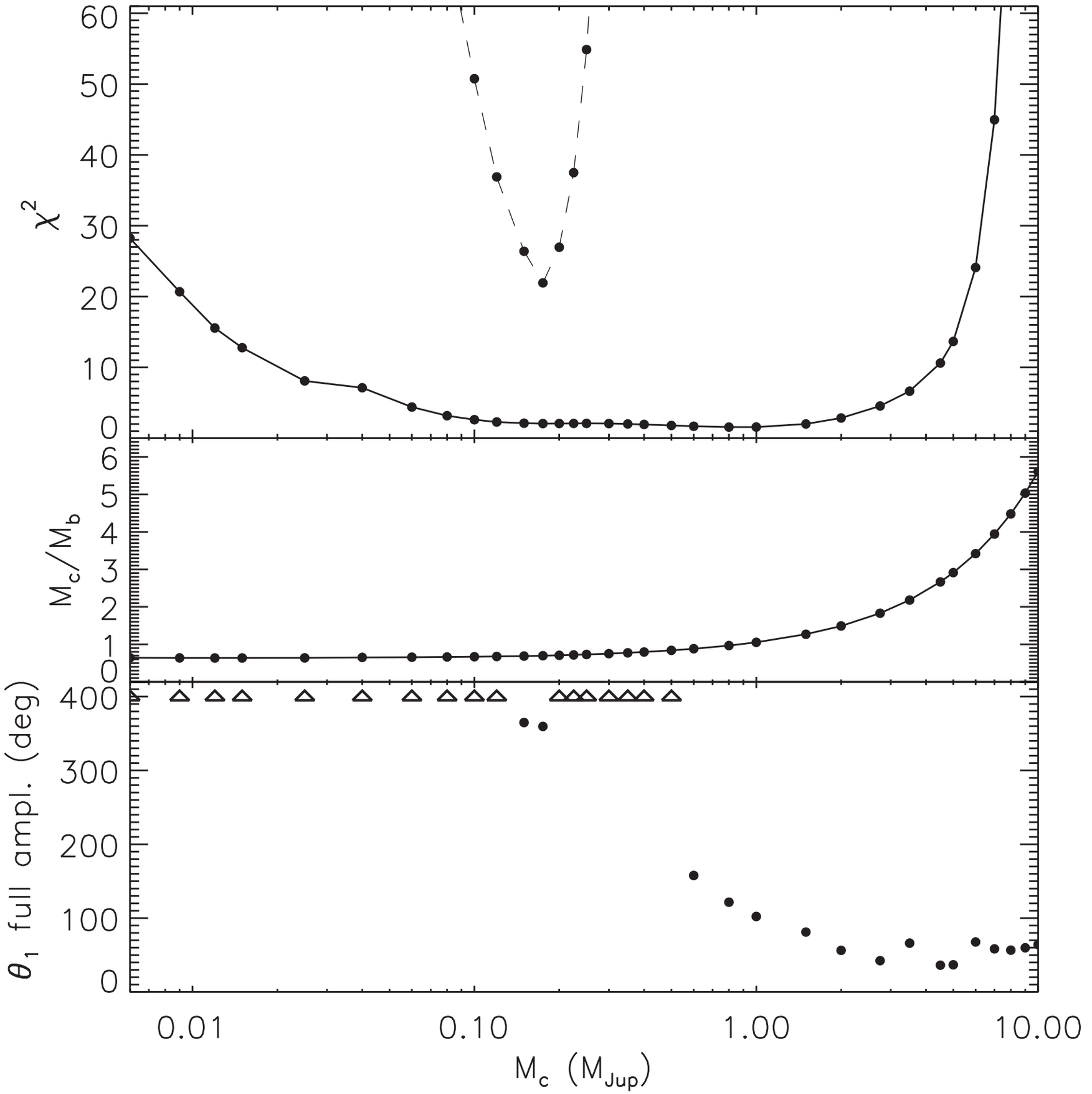
60
50
40
30
20
10
0
χ^2
6
5
4
3
2
1
0
M_c/M_b
400
300
200
100
0
θ_1 full ampl. (deg)
0.01
0.10
1.00
10.00
M_c (M_{Jup})

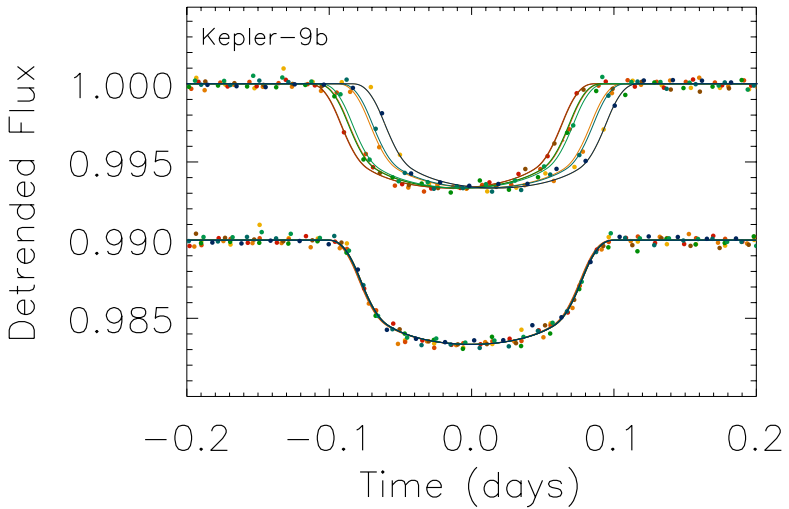
Kepler−9b
Detrended Flux
1.000
0.995
0.990
0.985
−0.2
−0.1
0.0
0.1
0.2
Time (days)

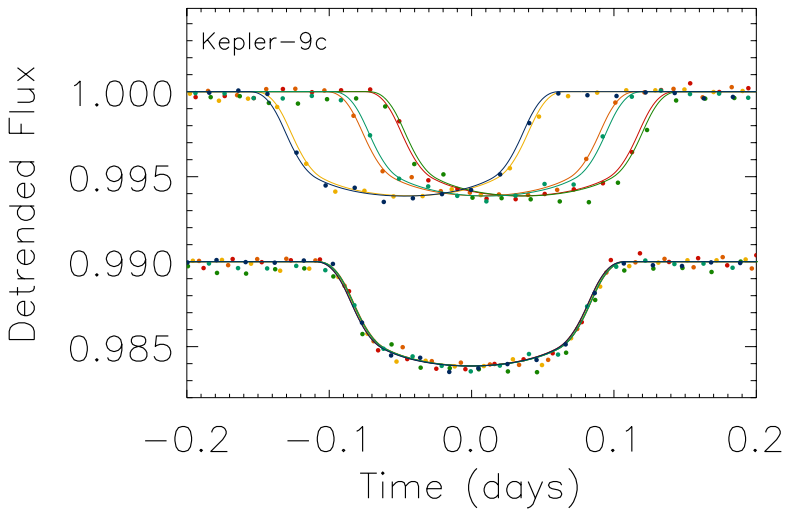
Kepler−9c
Detrended Flux
1.000
0.995
0.990
0.985
−0.2
−0.1
0.0
0.1
0.2
Time (days)

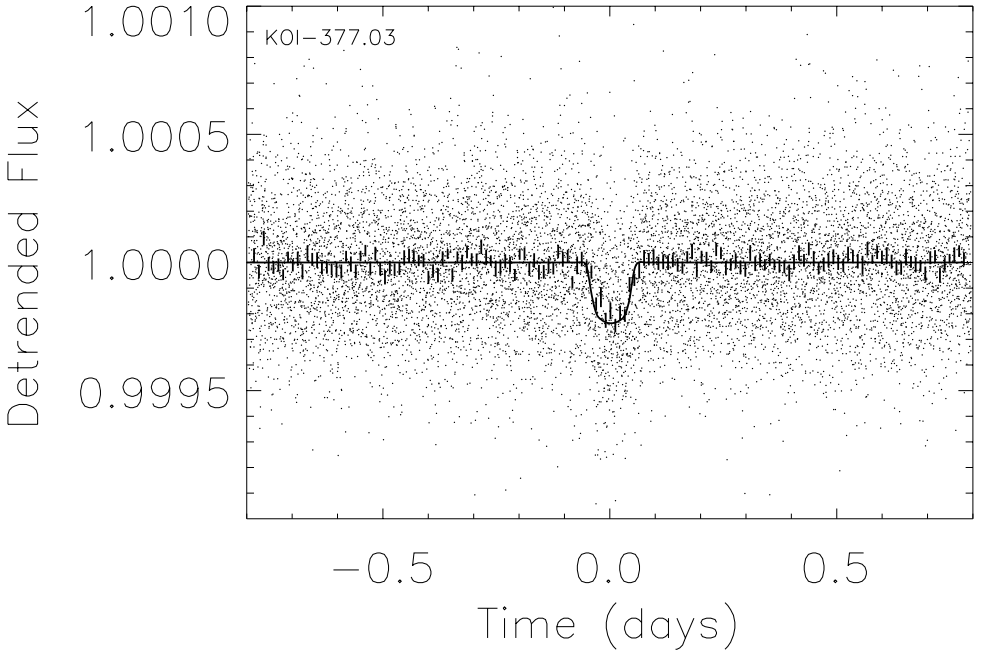
KOI−377.03
1.0010
1.0005
1.0000
0.9995
Detrended Flux
−0.5
0.0
0.5
Time (days)